JOURNAL OF GUIDANCE, CONTROL, AND DYNAMICS
Vol. 15, No. 2, March-April 1992

Improved Noise Rejection in Automatic Carrier Landing Systems

D. Joseph Mook,* Douglas A. Swanson,† and Michael J. Roemer‡
State University of New York at Buffalo, Buffalo, New York 14260
and
Roger Noury§
Bell Aerospace TEXTRON, Buffalo, New York 14240

A technique for reducing the effect of sensor noise in automatic carrier landing systems (ACLS) is developed. For demonstration purposes, the effect of radar noise on the altitude control portion of an ACLS is studied using digital computer simulation. A noise rejection filter, which blends model estimates of the plane's vertical velocity and acceleration with altitude information obtained by radar, is added to the tracking/control algorithm to decrease the sensitivity to noise. However, this results in an unacceptable increased sensitivity to turbulence. An optimization of the tracking/control gains is then performed to prevent degradation of the system's response to turbulence while simultaneously achieving high noise rejection and adequate transient response. In the simulation, a 90% improvement in noise rejection capability is achieved using the new tracking/control algorithm, without increased turbulence response.

Introduction

SENSOR noise usually creates problems in feedback control systems. Typically, the presence of sensor noise in the feedback loop produces high noise in the control signal if the control gains are high. If the gains are lowered to reduce the noise in the control signal, then closed-loop system stability is adversely affected due to decreased response speed (increased lag). Direct filtering of the sensor output may reduce the tradeoff between noisy control action and decreased stability, but in a limited fashion. In this paper, a technique is described that produces additional smoothing of the control action without adversely affecting system stability. A separate feedback loop containing a plant model is created, and its output is blended with the sensor data to provide less noisy control action without loss of stability.

To provide illustration on a detailed example, the technique is applied to automatic carrier landing systems (ACLS). The example is representative of a typical ACLS but is not intended to provide exact results for any particular plane/ACLS system. The typical ACLS is a fully automatic control system that provides flight control until touchdown on an aircraft carrier (see, e.g., Urnes and Hess[1] and Urnes et al.[2]). The system is composed of a shipboard radar tracking system, a digital computer, and a radio data link. The shipboard radar is used to measure the aircraft's position. The ship's digital computer then calculates corrective control commands, which are transmitted to the aircraft to directly control its position and orientation. The main goal of the system is to automatically control the aircraft in adverse conditions such as pilot fatigue, low visibility weather, heavy atmospheric turbulence, and/or deck motion caused by high seas.

Received Jan. 26, 1990; presented as Paper 90-3374 at the AIAA Guidance, Navigation, and Control Conference, Portland, OR, Aug. 20-22, 1990; revision received Oct. 23, 1990; accepted for publication Oct. 23, 1990.

*Associate Professor, Department of Mechanical and Aerospace Engineering. Member AIAA.

†Research Assistant, Department of Mechanical and Aerospace Engineering; currently at Lord Corporation, Cary, NC.

‡Research Assistant, Department of Mechanical and Aerospace Engineering; currently at Lord Corporation, Erie, PA. Member AIAA.

§Chief, Systems Engineering, P.O. Box 1; currently retired.

Although newer landing system designs usually use the plane's attitude, velocity, and/or acceleration sensors, and/or inertial navigation systems (INS), along with the remote radar tracking data, existing systems utilize only ship-based radar tracking data. Since radar measurements of the aircraft's position are the only inputs to the system, a major factor is the amount of noise contributed by the radar tracking system. Unfortunately, the dominant frequency range of the radar noise is concentrated in the same spectral region as the landing system's normal operating frequency. Radar noise leads directly to noisy control commands, resulting in a very bumpy approach for the pilot.

In this paper, we describe a modification of the tracking/control algorithm that can significantly reduce the sensitivity of the command signal to radar noise. The use of additional aircraft sensors, INS, etc., to reduce noise is not considered in this paper because such use would require costly hardware changes/additions. The approach of this paper could be implemented in the software of existing systems.

Computer simulations of the system with and without the noise rejection filter of this paper are constructed. The essential computer simulation blocks are the aircraft model, tracking filter, and controller. These simulation blocks are introduced, analyzed, and then combined in a closed-loop simulation to model an aircraft under ACLS control. The closed-loop performance is carefully analyzed in the frequency domain and time domain and compared with test flight measurements to ensure suitability of the simulation.

Because the landing approach normally involves small angles and minimal maneuvering, the equations of motion are decoupled in the design and implementation of the ACLS. Consequently, for space considerations, in this paper attention is restricted to the altitude control of the plane, achieved via pitch commands.

The proposed noise rejection filter uses both measurement data and modeled aircraft dynamics to produce a control signal that is less sensitive to radar noise. After the addition of this filter to the computer simulation, a complete frequency and time domain analysis is performed for comparison with the original system. From that analysis, a significant reduction in the levels of the noise in the control signal is observed. However, this desirable reduction is obtained at the cost of an undesirable increase in the turbulence response of the aircraft.

To lower the aircraft's response to turbulence while maintaining a high noise rejection in the pitch command, an opti-

mization technique is used to determine the gains in the control law and tracking filter as well as in the noise rejection filter. The optimization problem consists of the minimization of a cost function related to 1) the turbulence response of the aircraft, 2) the noise levels in the pitch command, and 3) the unit step response of the closed loop. Determination of an appropriate cost function is not trivial and is described in detail in a later section. The optimization cost function is constructed from simulated aircraft responses in the time domain, during ACLS-controlled flight through turbulence and in the presence of radar noise.

Description of Automatic Carrier Landing System

In this section, the operation of the closed-loop system is explained. A computer simulation for vertical (altitude) control is developed. For the purpose of organization, the simulation can be divided into three parts: the tracking filter, the controller, and the aircraft model.

A block diagram of the system designed to control the vertical position of an approaching aircraft is shown in Fig. 1. The system operates in the following manner. First, a radar measurement of the plane's position is obtained. A position error signal representing the difference between the plane's measured and desired altitude (*zer* in Fig. 1) is the input to the tracking filter. The tracking filter, described in detail in the following section, is a modified $\alpha - \beta - \gamma$ filter. The output of the filter consists of estimates of the aircraft's altitude error and the first and second derivatives of the altitude error. These filter output error estimates are used as inputs to a proportional, integral, derivative, and double derivative (P-I-D-DD) controller scheme. The controller produces a pitch command signal that is communicated to the aircraft to correct its vertical position. Then the position of the aircraft is once again measured by the radar system, and a new position error signal is generated and fed back to the controller. This closed-loop system operates until the aircraft has landed.

Tracking Filter

A modified $\alpha - \beta - \gamma$ filter[3] is used for tracking the approaching aircraft. The intent of the $\alpha - \beta - \gamma$ filter is to provide estimates of the plane's vertical position, velocity, and acceleration to the controller. The filter equations are derived in the following manner. First, a predicted position error $z_e^p(n)$ is derived using a discrete time, truncated Taylor series:

$$z_e^p(n) = z_e(n-1) + \Delta t \dot{z}_e(n-1) \tag{1}$$

where n denotes the current measurement time and $n-1$ denotes the previous measurement time. The predicted position error $z_e^p(n)$ and the measured position error $zer(n)$ are combined in the following manner to produce the filtered error signal $z_e(n)$:

$$z_e(n) = (1-\alpha)z_e^p(n) + \alpha zer(n) \tag{2}$$

where α is the filter gain used for the position measurement. In a similar fashion, the first derivative of the filtered error signal is calculated by combining the previous velocity estimate with a numerical estimate of the derivative:

$$\dot{z}_e(n) = (1-\beta)\dot{z}_e(n-1) + \beta\left[\frac{zer(n) - z_e(n-1)}{\Delta t}\right] \tag{3}$$

where β is the filter gain used for the velocity estimate. The acceleration section of the $\alpha - \beta - \gamma$ filter is separated into two equations. The first equation, a "predicted" second derivative of the position error, is written as

$$\ddot{z}_e'(n) = (1-\gamma)\ddot{z}_e(n-1) + \frac{\gamma}{\Delta t}[\dot{z}_e(n) - \dot{z}_e(n-1)] \tag{4}$$

where γ is the filter gain used for the acceleration estimate. The filtered error signal's second derivative is then calculated as

$$\ddot{z}_e(n) = \ddot{z}_e(n-1) + \gamma[\ddot{z}_e'(n) - \ddot{z}_e'(n-1)] \tag{5}$$

The implementation of the tracking filter is represented in Fig. 2.

The velocity (D) and acceleration (DD) error estimates are determined from numerically calculated derivatives of the position measurements. The examples in a later section show that the accuracy of the derivatives is highly sensitive to measurement noise. The effects of noise are amplified in the derivatives because the numerical differentiation is severely corrupted by opposite-sign measurement noise errors in successive measurements.

For stability, the controller uses D and DD action. However, the D and DD signals produced by the tracking filter are very noisy. System performance may be described as stable but "bumpy." Restated in this context, the primary objective of this paper is to reduce sensitivity to noise without sacrificing stability.

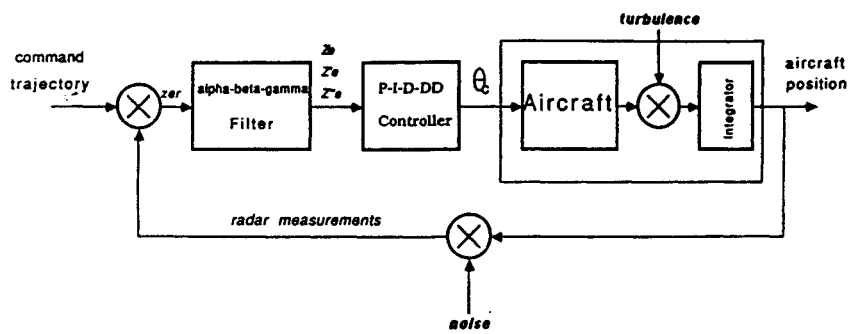

Fig. 1 Automatic carrier landing system block diagram.

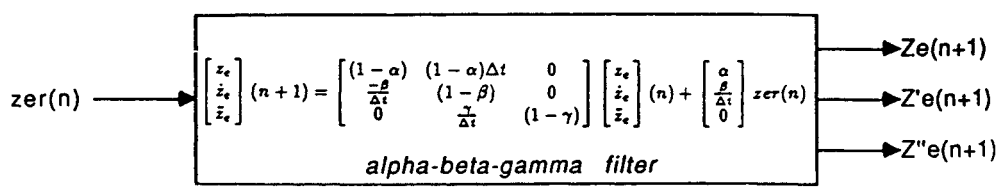

Fig. 2 Tracking filter block diagram.

Controller

The control law uses proportional (P), integral (I), derivative (D) and second derivative (DD) control action. In addition, a simple first-order low-pass filter, located at the output of the controller, attempts to smooth the control signal and prevent severely changing control signals from being transmitted to the aircraft. Moreover, limiters, notch filters, and other various features are used for special purposes in the control scheme. Deck motion compensation is also provided by the ACLS in the last few seconds before touchdown. Since the limiters, notch filters, and deck motion compensation system are not significant in determining new methods of reducing the noise content in the control signal, they are not considered in this paper.

The discrete time integral action is obtained by a numerical integration approximation, as shown in the following:

$$\Theta_{\mathrm{INT}}(n) = \Theta_{\mathrm{INT}}(n-1) + \frac{K_0}{K_I}\left[\frac{z_e(n) + z_e(n-1)}{2}\right]\Delta t \qquad (6)$$

where $\Theta_{\mathrm{INT}}(n)$ is the integral control action at the current discrete time, K_0 is a factored gain constant, and K_I is the integral control gain. The integral action is then used along with the filtered error signal and its derivatives to produce the following control signal:

$$\Theta_c'(n) = K_0[K_P z_e(n) + K_D \dot{z}_e(n) + K_{DD}\ddot{z}_e(n)] + \Theta_{\mathrm{INT}}(n) \qquad (7)$$

where $\Theta_c'(n)$ is the raw pitch command at time n, K_P is the proportional gain, K_D is the derivative gain, and K_{DD} is the double derivative gain. The calculated $\Theta_c'(n)$ control signal is then used as an input to a low-pass filter to produce the actual control signal $\Theta_c(n)$ given as follows:

$$\Theta_c(n) = \Theta_c(n-1) + \alpha_p[\Theta_c'(n) - \Theta_c(n-1)] \qquad (8)$$

where α_p controls the break point frequency.

The implementation of the controller is shown schematically in Fig. 3.

Aircraft Model

The construction of the aircraft model was based on actual aircraft data measured through flight testing. The measurements are of an F-4 fighter plane under ACLS control. The origin of the data is given in Ref. 4. Since the noise rejection approach of this paper is limited to the shipboard control

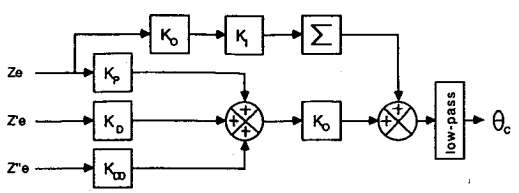

Fig. 3 P-I-D-DD controller block diagram.

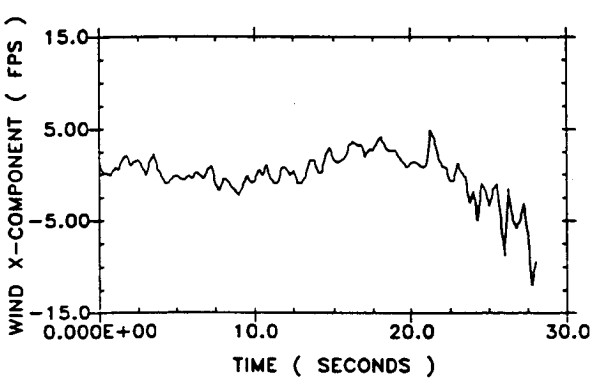

Fig. 4 Horizontal wind velocity data.

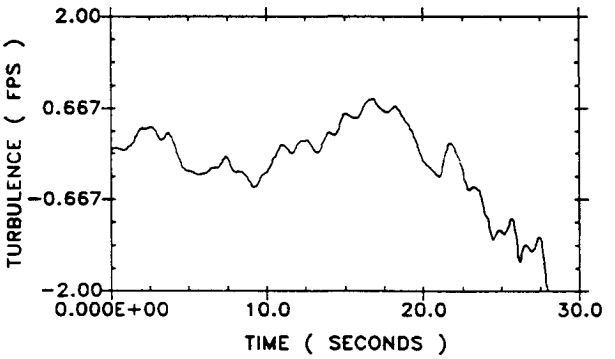

Fig. 5 Vertical plane velocity caused by turbulence.

algorithm and does not involve modification of any aircraft, the aircraft model should accurately represent the existing relationship between the transmitted pitch command and the altitude of the plane. The following transfer function, relating altitude to pitch command, closely models the actual flight data:

$$\frac{Z(s)}{\Theta_c(s)} = \frac{5.0}{s(1 + 1.4s)(1 + 1.0s)} \qquad (9)$$

where $Z(s)$ is the aircraft's altitude, and $\Theta_c(s)$ is the pitch command control signal. Equation (9) provides a good model of the plane's altitude response to pitch control commands and is used as the primary transfer function. Verification using the flight data is provided in the next section.

No attempt is made to model the internal states of the plane, as would be required if the ACLS modifications included modifications to the aircraft and/or aircraft-based control systems (autopilot, thrust compensator, etc.). The classical three-dimensional rigid-body equations of motion can be represented by a 12th-order state space model. However, if the plane's elasticity and control systems are included, the order of a state space representation increases without a theoretical upper bound.

Turbulence encountered by an aircraft under ACLS control is typically severe because under typical operation the ship is driven into the wind at fairly high speeds to minimize the relative velocity of the plane to the deck at touchdown. Turbulence is generated by wind blowing over deck structures and parked airplanes in addition to natural causes. Because of the availability of data, the effects of horizontal wind gusts on the vertical velocity of the plane along the glideslope is used as turbulence input to the simulation. Numerous experiments have been performed by Bell Aerospace to determine both the magnitude of the horizontal wind gusts along the plane's glideslope and the effects of these wind gusts on the plane's vertical position.[5] The wind velocity is determined from the following relation:

$$w_x = v_a + \dot{x} \qquad (10)$$

where w_x is the magnitude of the horizontal wind velocity along the glideslope, v_a is the plane's true horizontal airspeed, and $\dot{x}$ is the inertial horizontal closing speed.

The airspeed and closing speed were recorded during typical aircraft to ship approaches. The horizontal wind velocity was then indirectly determined from Eq. (10). This data set is shown in Fig. 4.

The effects of these horizontal wind velocity gusts on the plane's vertical velocity can be shown mathematically in the form of a frequency response transfer function. Since normal experimental methods for determining a frequency response transfer function rely on using sinusoidal inputs, and no sinusoidal wind gusts can be found, statistical methods must be used to calculate the transfer function. These methods are

based on the power and cross-spectral densities of the input and the output in the following manner:

$$T(j\omega) = \frac{S_{fx}(\omega)}{S_{xx}(\omega)} \tag{11}$$

where $T(j\omega)$ is the transfer function, $S_{fx}(\omega)$ is the cross-spectral density of the input $f(t)$ and the output $x(t)$, and $S_{xx}(\omega)$ is the power spectral density of the output $x(t)$. Magnitude and phase results are represented in the form of a Bode plot for several different aircraft passes in turbulent air. A mean transfer function was fit to the experiment data. This transfer function is

$$T(s) = \frac{Y(s)}{V(s)} = \frac{1.25s}{(1.67s + 1)(1.67s + 1)} \tag{12}$$

where $Y(s)$ is the vertical plane velocity, and $V(s)$ is the horizontal wind velocity. This transfer function is converted to a set of state equations that are numerically integrated to determine the change in the plane's vertical velocity due to a horizontal wind gust. Changes in the plane's vertical velocity corresponding to the horizontal wind velocity of Fig. 4 are shown in Fig. 5.

With turbulence included, the airplane model may be represented as shown in Fig. 6.

Characteristics of the Landing System

In this section, frequency and time domain analysis is performed to analyze the characteristics of the existing landing system (without the noise rejection filter) and to ensure that the computer simulation is an accurate model. To determine whether or not the closed-loop simulation accurately models the system, it must be compared with some actual test flight measurements.

Closed-Loop Frequency Domain Results

Through the use of a Nichol's chart, open-loop frequency test flight data were transformed into closed-loop magnitude and phase Bode plots. Next, magnitude and phase Bode plots of the closed-loop simulation were obtained. The results of the simulated frequency domain analysis are plotted together with the test flight data in Figs. 7 and 8.

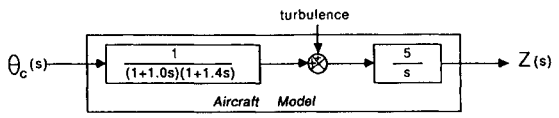

Fig. 6 Aircraft transfer function block diagram.

From the frequency response Bode plots in Figs. 7 and 8, the computer simulation provides a good model of the existing ACLS system. This simulation, matched with the F-4 flight data, shows a bandwidth of approximately 1.1 rad/s. These results are similar to those obtained by Urnes and Hess for an F/A-18 aircraft under control in which a closed-loop bandwidth of 1.2 rad/s was reported.[1]

Closed-Loop Step Response Results

An adequate step response of the aircraft is essential for efficient and safe operation of the system. For example, close to touchdown, a fast response and low overshoot are critical for a successful landing. Examining the step response of the simulation reveals an overshoot of 25.0%, a rise time of 6.7 s, and a settling time (±5% of steady-state value) of 20 s. The step response is shown in Fig. 9. This step response compared favorably with experimental data, not shown here, provided by Bell Aerospace.

Closed-Loop Turbulence Response Results

A practical representation of the operating conditions encountered by the system requires introduction of simulated radar noise and turbulence into the closed-loop simulation. As discussed previously, the turbulence is added directly to the aircraft model as a vertical velocity disturbance. Radar noise is represented by adding noise to the position measurements of the aircraft. To mimic this noise, a sinusoid of 4 rad/s is used as the noise input in the simulation. This model was chosen because 1) the effects of a sinusoidal input are easily seen in the pitch command signal, 2) the frequency of 4 rad/s is the approximate corner frequency of the combination $\alpha - \beta - \gamma$ filter and controller, and this produces the largest effect on the pitch command, and 3) the actual radar noise is usually dominated by electronic scintillation noise of approximately this frequency, although lesser random noise may also be present.

The closed-loop turbulence response of the aircraft is defined as the error in the position of the aircraft when only outside disturbances (noise and turbulence) affect the system. The simulated closed-loop system, when subjected to the noise and turbulence models, has the turbulence response shown in Fig. 10.

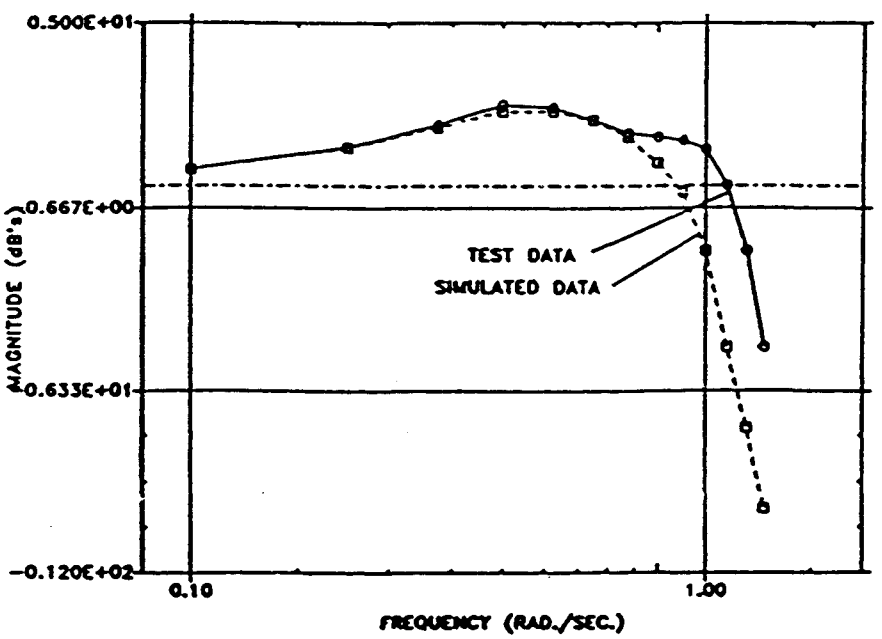

Fig. 7 Magnitude Bode plot comparison.

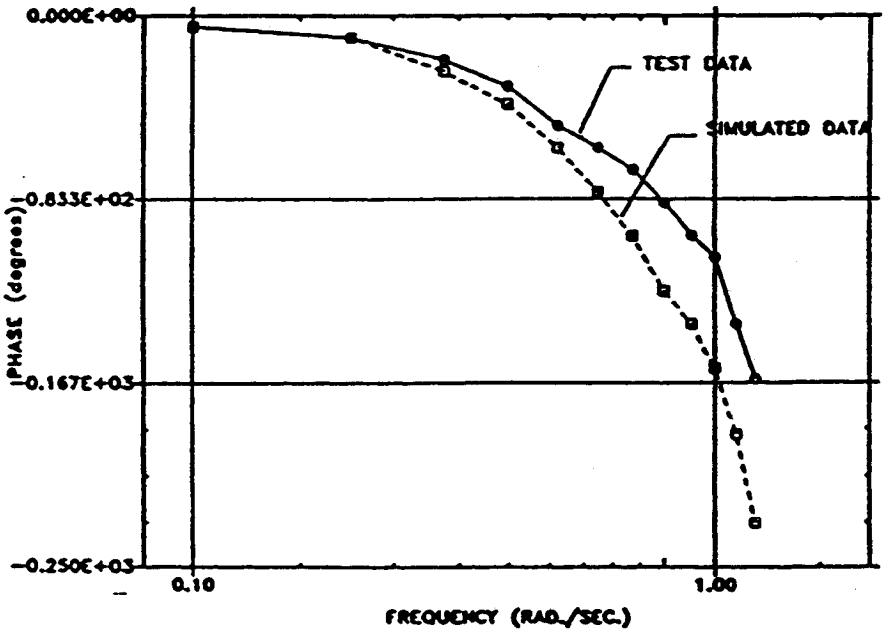

Fig. 8 Phase Bode plot comparison.

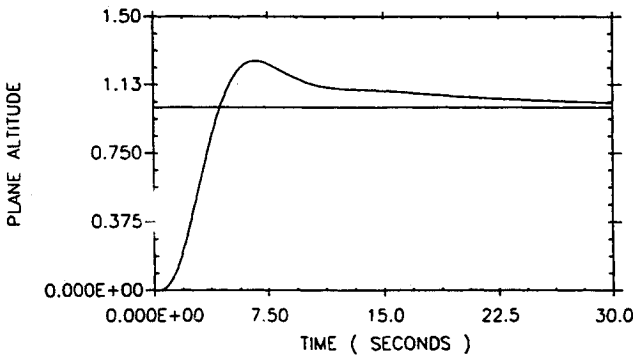

Fig. 9 Closed-loop step response.

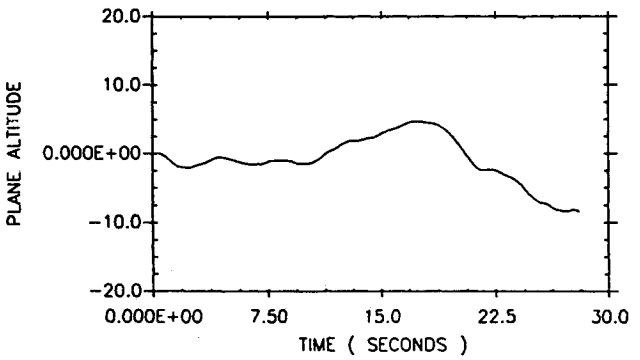

Fig. 10 Turbulence response of the closed-loop simulation.

Noise Rejection Filter Analysis

The primary incentive for adding a noise rejection filter to the system is to reduce the amount of noise present in the control signal, thereby producing more stable motions in the aircraft's response. The pitch command noise often produces an undesirable jerking motion in the control system.

The noise rejection filter blends radar altitude measurements with model estimates of the aircraft's velocity and acceleration to produce an error signal that is less sensitive to radar noise. The aircraft model estimates are produced from the numerical integration of the model previously developed. A Laplace transfer function representation of the noise rejection filter is

$$Y(s) = \frac{X(s) + A\hat{x}(s) + B\hat{\hat{x}}(s)}{1 + As + Bs^2} \tag{13}$$

where $Y(s)$ is the noise rejection filter output (vertical position), $X(s)$ is the measured position data, $\hat{x}(s)$ is the velocity estimate from the aircraft model, $\hat{\hat{x}}(s)$ is the acceleration estimate from the aircraft model, and A and B are variable gains of the filter.

The implementation of the filter's equations can be described in the following manner. The control signal sent to the aircraft is sampled at a rate of 20 samples per second and used as input to the aircraft model. The model in turn produces estimates of the vertical velocity and acceleration of the aircraft. The estimates and position measurements are blended together using a time-domain equivalent of the second-order filter algorithm of Eq. (13) to produce an error signal that is less sensitive to measurement noise. The improved error signal creates a "smoother" control signal that yields a more stable aircraft motion. The position of the noise filter with respect to the regular closed-loop system is illustrated in the block diagram given in Fig. 11.

The parameters A and B of the noise filter are chosen to minimize the amount of noise present in the control signal, while allowing the motion of the aircraft due to turbulence to pass through. These parameters directly affect the relative amount of measurement or estimate present in the blended error signal. For example, if A and B are large, the modeled aircraft dynamics become the dominant factor in the blended error signal. However, for smaller values of A and B, the emphasis is placed on the position measurements. Care must be taken, however, in choosing A and B since closed-loop characteristics such as step response and turbulence response can be degraded by the improper selection of the noise rejection filter gains.

As a first approximation in determining the filter gains, the bandwidth of the noise rejection filter is matched with the bandwidth of the aircraft transfer function. Thus, modeling a system with ω equal to 1 rad/s and a damping ratio of 0.7 produces the parameters $A = 1.4$ and $B = 1.0$.

An example illustrating the noise rejection capabilities of the proposed filter is shown in Figs. 12 and 13. First, using only noise as the input disturbance, a command signal of zero is directed to the aircraft. A plot of the input noise, control signal, and aircraft response for the current system (no noise

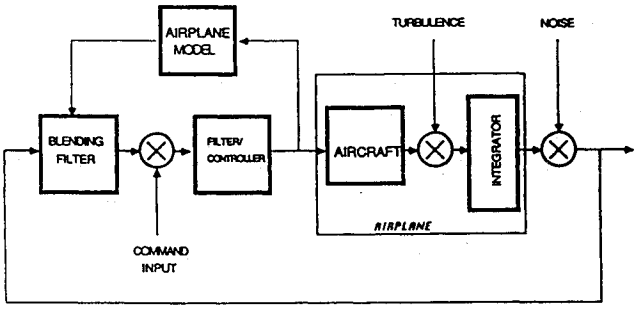

Fig. 11 Closed-loop block diagram with noise filter.

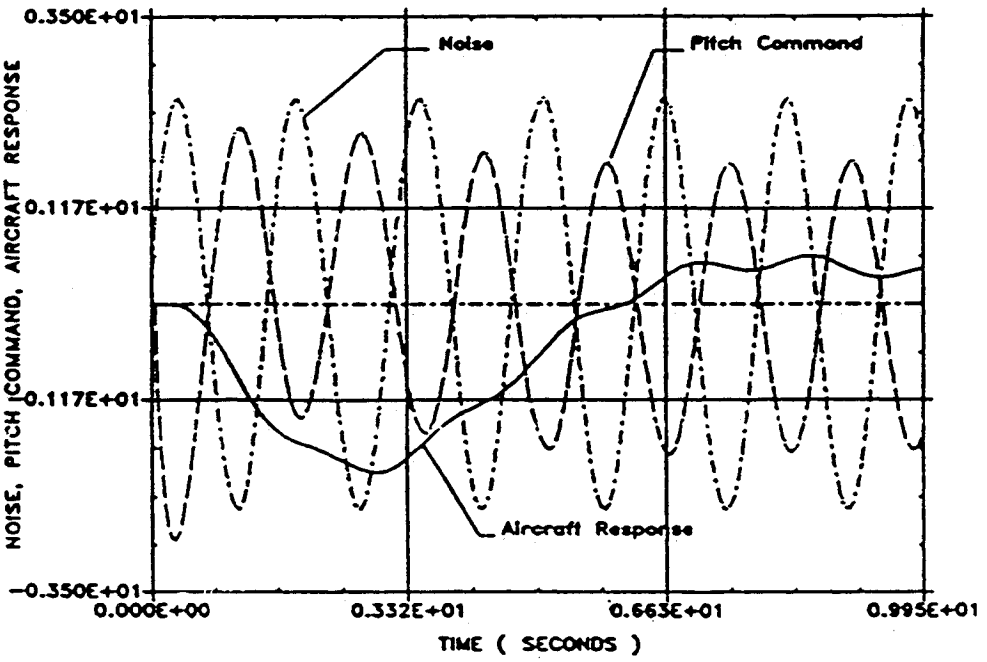

Fig. 12 Disturbance response without noise filter.

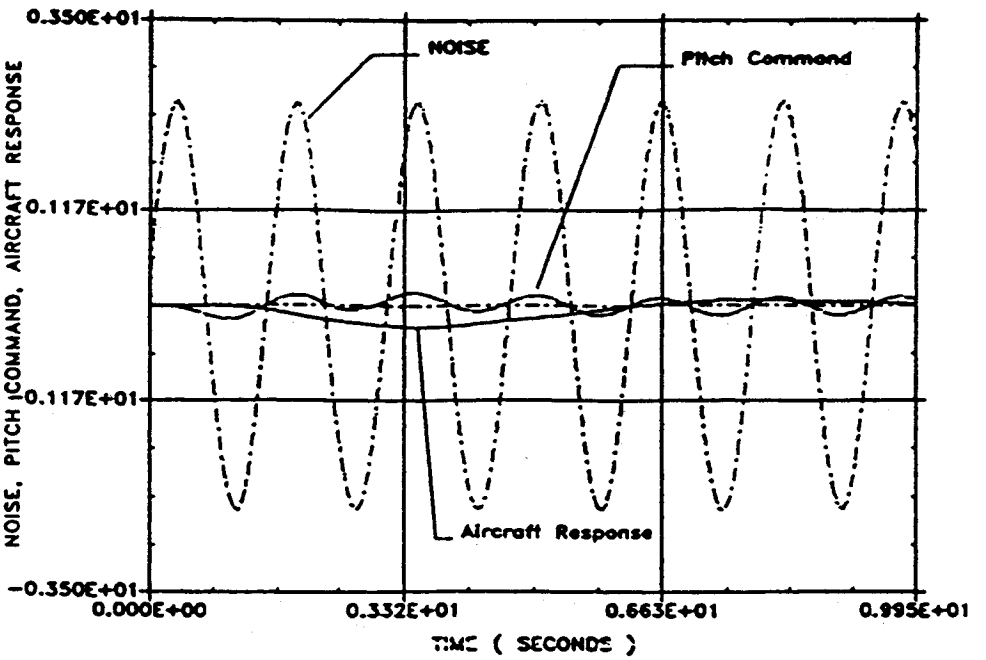

Fig. 13 Disturbance response with noise filter.

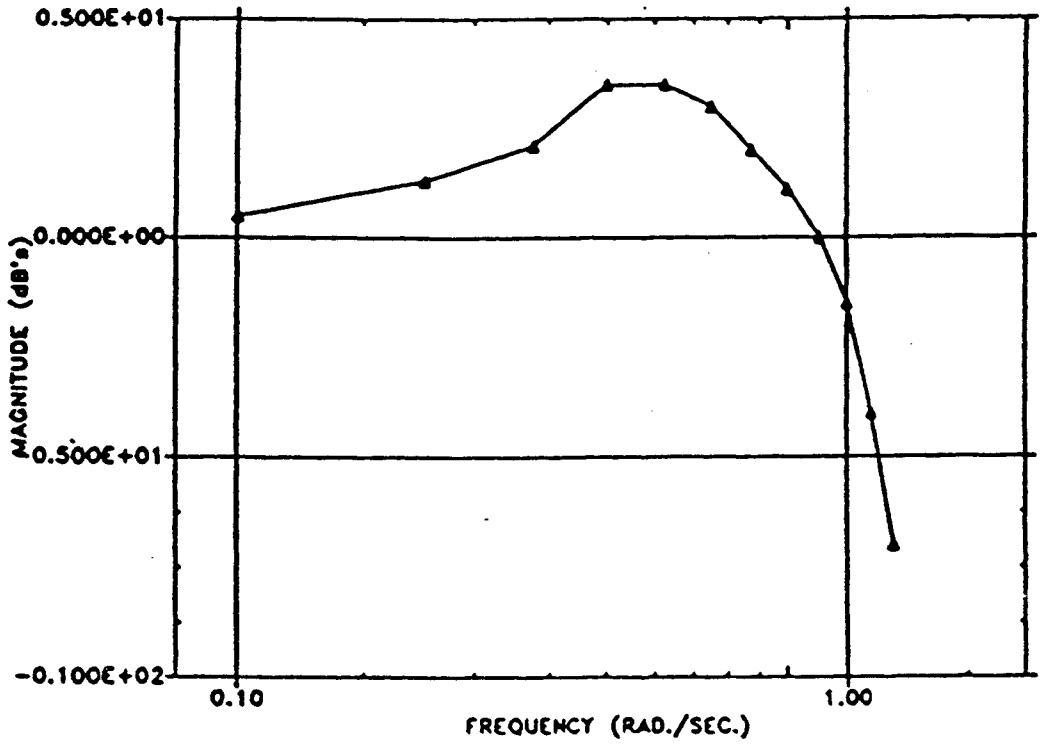

Fig. 14 Closed-loop magnitude Bode plot (with filter).

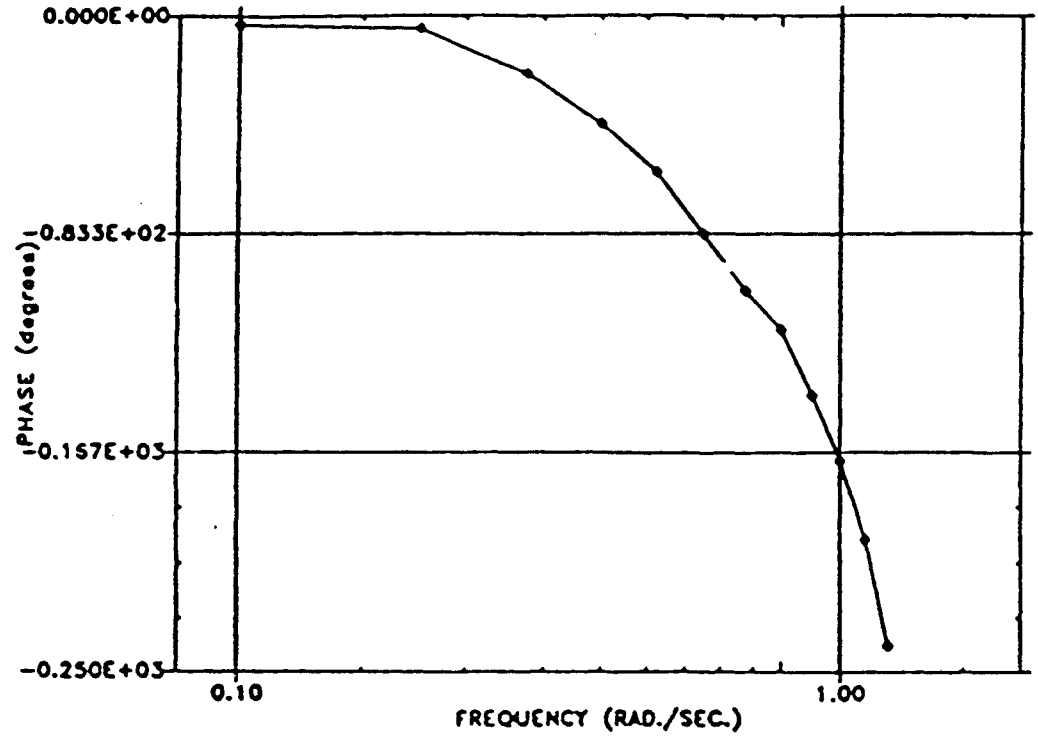

Fig. 15 Closed-loop phase Bode plot (with filter).

Table 1 Simulation comparison

	Original system	System with filter
Gain margin, dB	4.2	4.3
Phase margin, deg	40	45
Bandwidth, rad/s	1.1	1.2
Gain at ω_p, dB	2.5	3.0

rejection filter) is shown in Fig. 12. Next, under identical conditions, the simulation including the noise rejection filter is tested, and the results are given in Fig. 13. The ability of the noise rejection filter to reduce noise in the pitch command and thus smooth the motion of the plane is clear from comparing the results of Figs. 12 and 13.

System with Noise Rejection Filter

In this section, frequency and time domain analysis is performed to determine the effects of the addition of the noise rejection filter on the closed-loop frequency and time domain responses of the system.

Closed-Loop Frequency Domain Results (with Noise Rejection Filter)

To further examine the properties of the system with the noise rejection filter, a frequency domain analysis is per-

formed. Magnitude and phase Bode plots of the closed-loop response (altitude response to an altitude command) is shown in Figs. 14 and 15.

The results of a magnitude and phase Bode plot comparison of the regular simulation and the simulation with the noise rejection filter are summarized in Table 1. These results show a slight increase in the magnitude response of the system.

Closed-Loop Step Response Results (with Noise Rejection Filter)

The results of the previous section, showing an increase in the magnitude Bode plot, suggest that the step response of the system might also be magnified with the addition of the noise rejection filter. This was found to be true, as shown in Fig. 16.

A comparison between the step response of the original system with that of the system with the noise rejection filter is shown in Table 2.

Closed-Loop Turbulence Response (with Noise Rejection Filter)

Examination of the increased frequency and step responses of the system with the noise rejection filter suggests that the turbulence response is also magnified. In fact, the turbulence response, using the identical noise and turbulence disturbance inputs, is increased by almost a factor of two. The turbulence response, with the noise rejection filter, is shown in Fig. 17.

Comparison of Figs. 10 and 17 demonstrates that despite the successful reduction of the noise sensitivity of the control signal, the addition of the noise rejection filter causes the aircraft to exhibit much greater motion when subjected to turbulence. This characteristic is unacceptable as turbulence response is a major concern during normal operations.[1] Therefore, the problem of how to reject noise and simultaneously prevent an increase in the turbulence response is now addressed. The approach taken in this paper, discussed in detail in the following section, is to alter all the control and filter gains of the system.

Control/Filter Variable Optimization

A technique is now developed that allows for the use of the noise rejection filter by lowering the turbulence response while

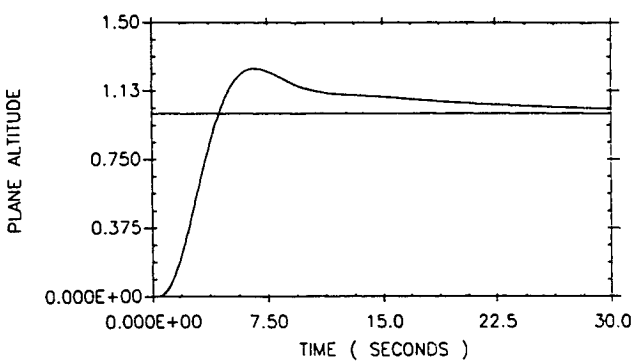

Fig. 16 System step response (with filter).

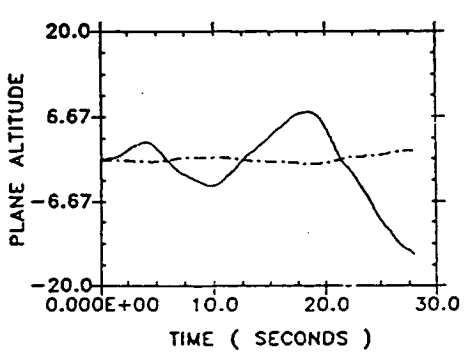

Fig. 17 Turbulence response with the noise filter.

Table 2 Step response comparison

	Original system	System with filter
Overshoot, %	25.0	28.0
Rise time, s	6.7	6.7
Settling time, s	20.0	25.0

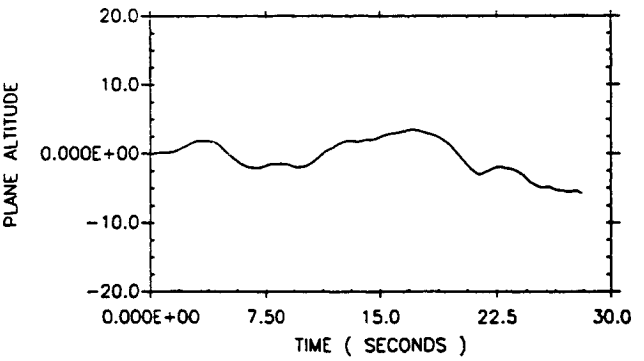

Fig. 18 Turbulence response for optimal control gains.

maintaining a high noise rejection in the control signal. An optimization approach is used that treats the errors in the aircraft's response as a cost function and the controller and filter gains as the variables to be optimized. A conjugate gradient direction extremization algorithm developed by Fletcher and Reeves[6] is used to formulate the optimization program that calculates the optimal gains for the landing system. The variables of optimization consist of the gains α and β from the tracking filter; the gains K_I, K_P, K_D, and K_{DD} from the controller; and the gains A and B from the noise rejection filter.

As in any complicated system with several, possibly competing, goals to be achieved, proper choice of the cost function is critical and yet difficult. Numerous approaches to choosing a cost function are described with numerical evidence of their subtle and not-so-subtle advantages and disadvantages.

Optimization of Turbulence Response

The turbulence response is defined as the aircraft's response with only outside disturbances (noise and turbulence) acting on the system. Since the desired error signal of the aircraft is zero, and position error is defined by $z_e(t)$, the turbulence cost function must include a penalty term for nonzero $z_e(t)$. The noise levels in the pitch command also must be penalized, but it is far less obvious how to construct a reasonable penalty since the pitch command necessary to offset turbulence is neither zero nor periodic. Through trial and error, it was found that the pitch command noise can be reduced by including terms proportional to both the pitch command and also the second derivative of the pitch command. The term proportional to the pitch command maintains the magnitude of the control signal at acceptable levels, while the term proportional to the second derivative of the pitch command reduces the high-frequency components. Adequate responses could not be obtained without using both terms. A quadratic form of the cost function is used to ensure a "well-defined" minimum and also to offset the positive and negative portions of the response. The cost function minimized to reduce both the turbulence response and the noise levels in the pitch command is

$$\Phi_{\text{turb}} = \int_{t_0}^{t_f} [W_1 z_e^2(t) + W_2 \Theta_c^2(t) + W_3 \ddot{\Theta}_c^2(t)]\, dt \qquad (14)$$

where $z_e(t)$ is the vertical position error of the aircraft, $\Theta_c(t)$ is the pitch command, and $\ddot{\Theta}_c(t)$ is the second derivative of the pitch command. The variables W_1, W_2, and W_3 are weighting factors that reflect the relative importance between obtaining

a low turbulence response and obtaining high noise rejection. Using trial and error, the values of $W_1 = 1$, $W_2 = 2$, and $W_3 = 5$ gave the best results in the optimization of the turbulence response. The turbulence response found by optimizing the cost function of Eq. (14) is shown in Fig. 18.

Comparing Figs. 10 and 18, the turbulence response of the original system is preserved while maintaining high noise rejection in the pitch command. These results are obtained by considering only the turbulence and noise responses. However, this particular change in control/filter gains produces a more oscillatory step response, shown in Fig. 19. Therefore, the next section addresses the problem of increased oscillations by optimizing the step response.

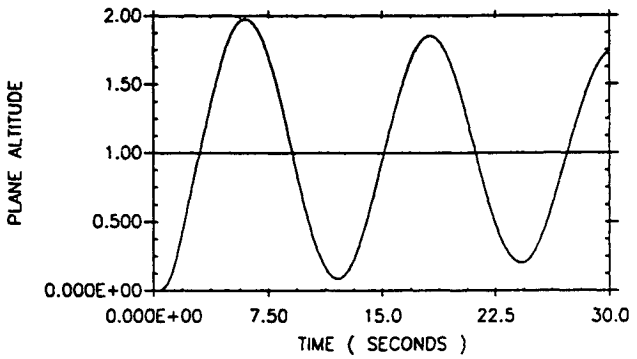

Fig. 19 Oscillatory step response.

Optimization of Step Response

By simply minimizing a cost function representative of only the turbulence and noise responses, the closed-loop transient characteristics of the system can easily be degraded. Therefore, attention is focused on obtaining an optimal step response so that transient closed-loop properties are acceptable. A desirable step response includes 1) a fast response time, 2) a low overshoot, and 3) a reasonable settling time. Initially, a cost function of

$$\Phi_{\text{step}} = \int_{t_0}^{t_f} [1.0 - z(t)]^2 \, dt$$

was chosen to achieve a desirable response. However, minimizing such an index by itself usually produces oscillatory behavior, which must be dampened. A cost function that takes

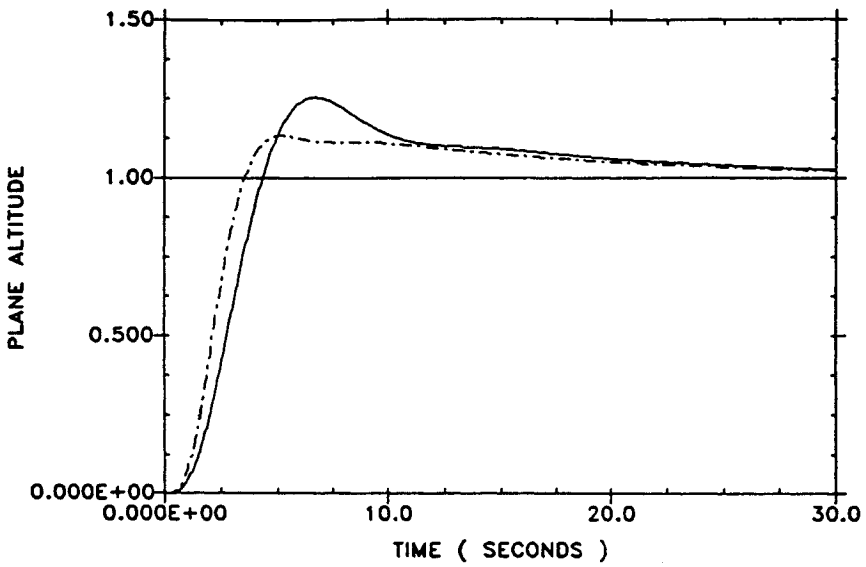

Fig. 20 Step response comparison for original and optimal gains.

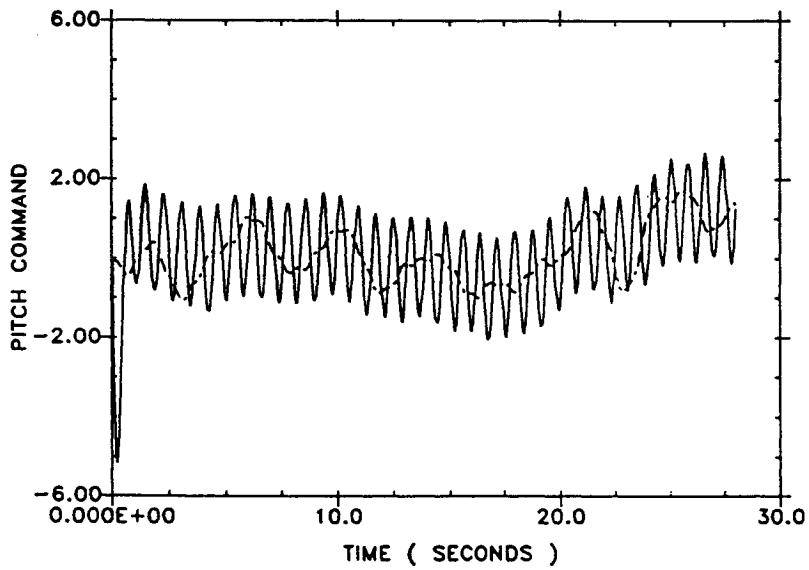

Fig. 21 Combined cost function noise levels.

into account all of these requirements is illustrated as follows:

$$\Phi_{\text{step}} = \int_{t_0}^{t_f} W_4[1.0 - z(t)]^2 + W_5\ddot{\Theta}_c^2(t)\,dt \qquad (15)$$

The first term in the cost function penalizes deviations from unity, producing a fast response. The second term provides for adequate damping. The values for W_4 and W_5 used in the optimization of the step response, obtained via trial and error, are $W_4 = 1$ and $W_5 = 2$. Implementing this cost function in place of the minimal turbulence response cost function yields the control and filter variables for an optimal step response. The step response with the noise filter are plotted for the original and optimal gains in Fig. 20 to illustrate the significant improvements.

However, the gains that produce the optimal step response severely degrade the turbulence response (not shown).

Combined Cost Function

As shown, optimizing a cost function that is solely representative of one particular aspect of the response degrades other critical characteristics related to the performance of the system. Therefore, a more encompassing cost function that includes both the turbulence response and the step response in addition to noise rejection is developed. This cost function is of the following form:

$$\Phi = W_6\Phi_{\text{turb}} + W_7\Phi_{\text{step}} \qquad (16)$$

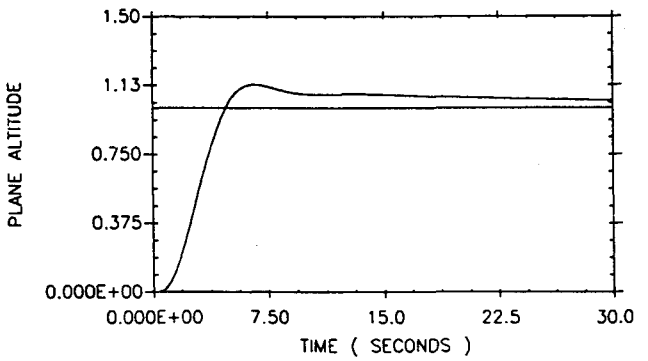

Fig. 22 Combined cost function step response.

where Φ_{turb} is defined in Eq. (14) and includes the noise rejection, and Φ_{step} is defined in Eq. (15). Proper weighting of each part must exist for obtaining a desired optimal response. The value of the cost function used in minimizing the turbulence response is numerically much greater than the cost function used in optimizing the step response. For this reason, a value of 1 for W_6 and a value of 200 for W_7 in the optimization of the combined cost function was found to produce filter/controller gains that lead to excellent noise rejection over the current system without seriously degrading the turbulence response. The improved noise rejection (a 90% reduction in the rms noise levels) is shown in Fig. 21.

The step response found by the combined cost function optimization is shown in Fig. 22, and the turbulence response is shown in Fig. 23. From these results, it is clear that the 90% reduction in noise sensitivity may be obtained without a corresponding degradation in the turbulence response.

Although not a direct motivation of the present work, the step response has also been improved (faster rise time with less overshoot than the original system).

Conclusions

In this paper, a technique for reducing the effect of sensor noise in the control action of a closed-loop system is developed. A typical automatic landing system was simulated and analyzed so that performance with respect to radar tracking and control could be evaluated. Noise levels in the radar measurements produce a noisy pitch command that is undesirable for many reasons, including stability and pilot comfort. Therefore, the noise rejection capability of the system was studied. A noise rejection filter was introduced that successfully produced excellent noise rejection abilities, at the expense of an increased turbulence response of the aircraft. An optimization program was then developed to minimize the turbulence response of the aircraft with respect to the system's control and filter variables, but this produced an undesirable step response and eliminated the improvements in the noise rejection. Finally, a cost function related to the turbulence, noise, and step responses was used to optimize the control and filter gains of the system. Employing these optimal gains into the system's control and filter algorithms produced excellent radar noise rejection (approximately 90% reduction from the current system) while preserving a normal turbulence response. Although not a goal of the present work, the unit step response was also improved over the current system.

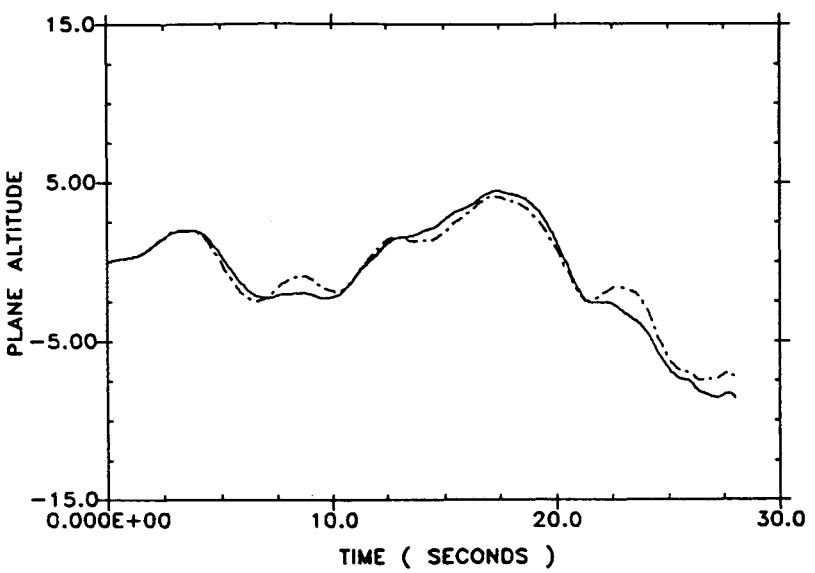

Fig. 23 Combined cost function turbulence response.

References

[1]Urnes, J. M., and Hess, R. K., "Development of the F/A-18A Automatic Carrier Landing System," *Journal of Guidance, Control, and Dynamics,* Vol. 8, No. 3, 1985, pp. 289–295.

[2]Urnes, J. M., Hess, R. K., Moomaw, R. F., and Huff, R. W., "H-Dot Automatic Carrier Landing System for Approach Control in Turbulence," *Journal of Guidance and Control,* Vol. 3, No. 2, 1981, pp. 177–183.

[3]Fitzgerald, R. J., "Simple Tracking Filters: Steady State Filtering and Smoothing Performance," *IEEE Transactions on Aerospace and Electronic Systems,* Vol. AES-16, No. 3, 1980, pp. 860–864.

[4]Roemer, M. J., "Robust Tracking and Control Strategies for Automatic Landing Systems," *Transportation Research Record,* No. 1257, Transportation Research Board of the National Research Council, 1990, pp. 30–43.

[5]"Automatic Carrier Landing System Computer Program Improvements," Bell Aerospace Textron, Final Rept. 6500-927243, Buffalo, NY, Feb. 1982.

[6]Fletcher, R., and Reeves, C. M., "Function Minimization by Conjugate Directions," *Computer Journal,* Vol. 7, No. 2, 1964, pp. 149–154.